Numerical simulations of synthetic jets in aerodynamic applications

Alexandru Catalin MACOVEI*,[1], Florin FRUNZULICA[2]

*Corresponding author
*,[1]Fokker Engineering Romania
Sos. Pipera 1/VII Nord City Tower, Voluntari, Ilfov, Romania
alexandru_macovei@yahoo.ro;
[2]"POLITEHNICA" University of Bucharest, Faculty of Aerospace Engineering
Polizu 1-6, RO-011061, Bucharest, Romania
ffrunzi@yahoo.com.

DOI: 10.13111/2066-8201.2014.6.S1.9

Abstract: *This paper presents numerical simulations of synthetic jets in aerodynamic applications. We've analyzed the formation of isolated synthetic jets, the influence of nozzle geometry and the interaction of synthetic jets with a uniform flow on a flat plate. Also we've studied the influence of the active control in interaction with a stalled airfoil and the controllability of dynamic stall phenomenon. The results are obtained using a dedicated CFD solver. Appropriate comparisons are made with results from scientific literature; as well the numerical results are compared with a set of experimental images.*

Key Words: *synthetic jet, actuator, flow control, active control, dynamic stall, boundary layer*

I. INTRODUCTION

A relatively new device for controlling the flow, produced and tested in the laboratory, is known as "synthetic jet actuator". Synthetic jets are produced by a sound source which is at the base of a cavity communicating with the surface exposed to the flow through the circular orifice, as seen in Figure 1.

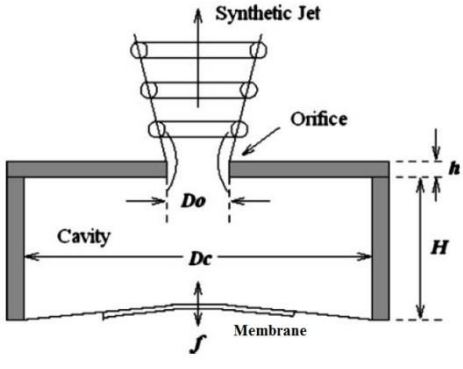

Figure 1. The conceptual scheme of synthetic jet actuator [3]

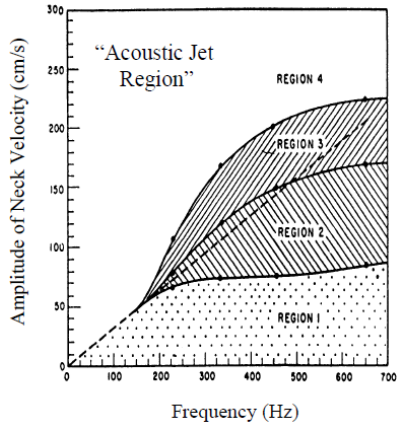

Figure 2. Zoning of acoustic jets [3]

The actuator is composed of a rigid-walled chamber, an inlet in the upper part exposed to the exterior flow and an elastic membrane which is opposite the orifice. In the phase in which the membrane moves down ward, the outside fluid is drawn into the cavity through the opening. When the membrane moves up, the fluid is discharged through the opening back to the outside flow. If the jet has sufficient energy a vortex ring is generated.

When the cycle is repeated periodically, a vortices column is generated. Sintered synthetic jet adds momentum to the fluid from the outside flow, this happens without added flux mass. Therefore synthetic jets are preferred at the expense of conventional jets.

At a high level of excitation of the elastic membrane, represented by the maximum amplitude of the membrane displacement, it is observed the emanation of a regular fluid jet. Because there is no additional contribution of mass, the stream lines should form a closed circulation as shown in Figure 1. This phenomenon of acoustic jet stream through an orifice which is based on a highly excited acoustic diaphragm is well known for many years. Figure 2, [3], shows the four regimes of circulation and turbulence around an acoustically excited orifice plate in terms of acoustic neck velocity (amplitude) versus frequency. The dotted line corresponds to the area where the particle displacement amplitude is equal to the length of the aperture hole.

At a low excitation level in region 1 and region 2, under the dotted line, a small amount of fluid particles are moving into and out of the cavity without interfering with the fluid outside the cavity. A small amount of acoustic energy is lost to the outside by the phenomenon of acoustic radiation.

Near and above the dotted line, in region 3, significant turbulence are generated near the neck of the orifice, however, a part of the acoustic energy is transferred to the fluid particles.

At high excitation levels, in region 4, the movement of the fluid particles extends beyond the opening providing sufficient time for the particles to form a vortex ring, with a circular aperture. This vortex is separated from the region of the orifice and cause a disturbance powered by the movements caused by convection vortex, thus synthetic jets are formed. All simulations done in this study are made so that the combination of amplitude and frequency should be in region 4.

In the last two decades the synthetic jets and the flow mechanism of its interaction with a cross-flow have been intensively investigated numerically and experimentally.

The advantage of these jets is that they can transfer linear momentum to the main flow without mass injection.

Synthetic jets cover a large range of time and length scales and thus can be attractive for many applications: the flow control of the boundary layer separation, command systems with jets, thrust vectoring, flow control on wind turbines, forced air cooling.

The present work is organized around the following problems: the generation of the synthetic jet, main parameters that characterize synthetic jet performances, the interaction of the synthetic jet with laminar boundary layer, and the effect of synthetic jet on the dynamic stall phenomenon. All investigations are performed numerically using ANSYS FLUENT.

II. GENERATION OF SYNTHETIC JETS

This study proposes the development of sets of numerical simulations at different frequencies and amplitudes of oscillation of the elastic membrane. The actuator has a fixed geometry with the following dimensions:

$$D_0 = 5\ mm \qquad h = 5\ mm \qquad D_c = 45\ mm \quad H = 10\ mm$$

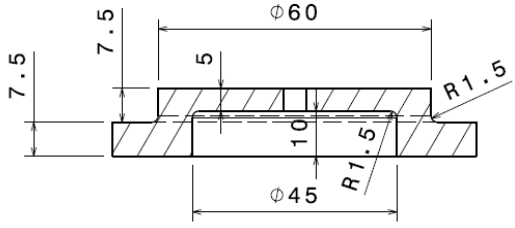

Figure 3 Synthetic jet actuator nozzle

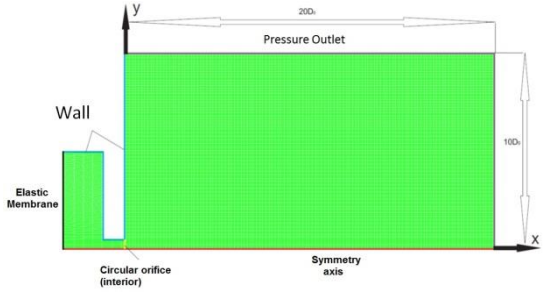

Figure 4. Computational domain and mesh

Any numerical results depend on the grid and the computational domain. For validation of a numerical simulation it is necessarily to prove that results are independent on the grid. In this work the numerical simulations were performed using two different grids. The differences between the results obtained with a grid containing 54000 and the results obtained with a grid containing 216000 elements are negligible.

Consequently, the simulations will be conducted using the grid with fewer elements in order to increase the calculation speed and to minimize the space required to store the results.

The numerical simulations are performed in ANSYS Fluent 13. An incompressible pressure solver based on a second order SIMPLE algorithm is utilized. The simulations are non-stationary and the problem is axially symmetric.

The laminar flow model is used; the working fluid is considered to be air having standard properties. To simulate the movement of the membrane the dynamic grid option is used. The motion law is implemented using a UDF.

The time step varies with the membrane oscillation frequency $\Delta_t = \frac{1/f}{200}$ where f is the frequency. Figure 5 and Figure 6 present the results of numerical simulations. The sequences reveal the vorticity at different moments of time.

The results in Figure 5 are obtained for a frequency f= 50Hz and an amplitude Δ= 0.4 mm. It is noted that the synthetic jet is weak for this combination of frequency and amplitude.

Instead, the results presented in Figure 6 are obtained for f = 400 Hz and an amplitude Δ= 0.8 mm.

The amplitude of the velocity is much higher than the speed of the former case, which leads to the complete development of synthetic jet, thus demonstrating the validity of the graph shown in Figure 2.

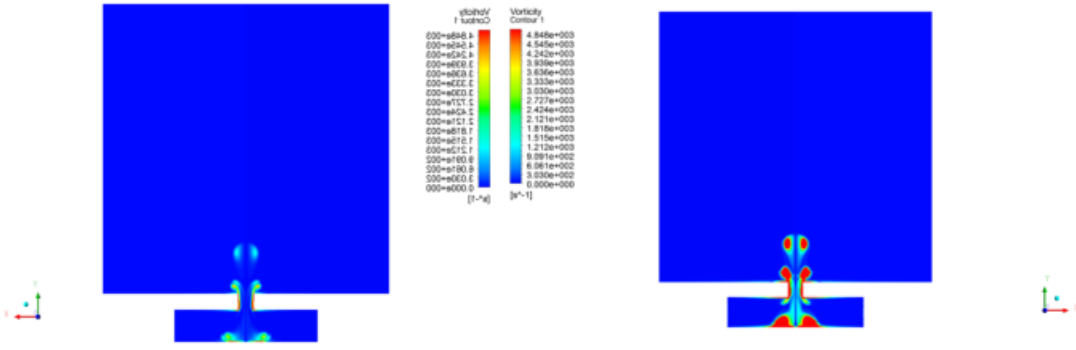

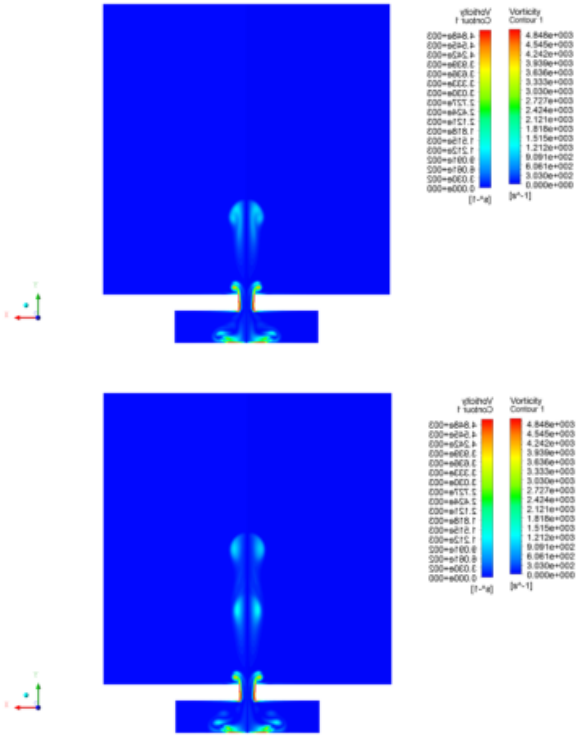

Figure 5. Synthetic jet vorticity contours for 50 Hz frequency

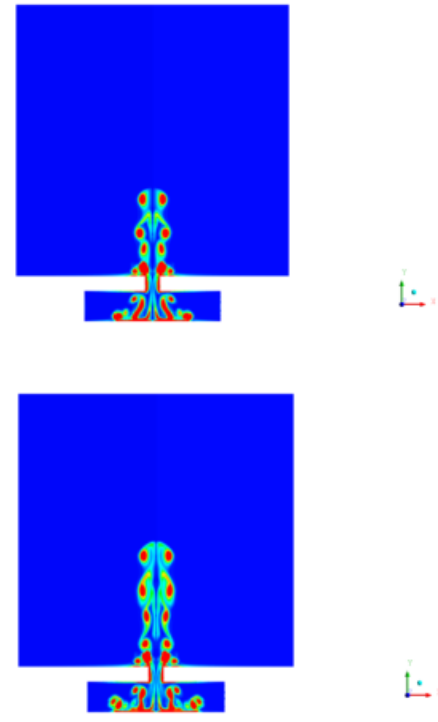

Figure 6. Synthetic jet vorticity contours for 400 Hz frequency

The magnitude of speed is higher than the speed of the previous case, which leads to the complete development of the synthetic jet, thus demonstrating the validity of the graph shown in Figure 2.

III. PARAMETERS WHICH DESCRIBE THE PERFORMANCE OF THE CIRCULAR SYNTHETIC JETS

The synthetic jets are characterized by the formation of vortex rings. The power of a vortex ring, in terms of the intensity of circulation, determines its impact on the boundary layer.

In order to ensure that the vortex rings have the strength to affect the boundary layer, it is necessary to know the parameters that influence the formation and propagation of the se vortex rings.

In terms of concept, it is of interest to be highlighted how the actuator geometry can be optimized to enhance the power of the vortex rings.

The study is based on the consideration that the membrane is embedded around the circumference.

Simulations are performed for different fixed values of amplitude and frequency. According to the theory of plates [13], the deformation of the membrane can be described by the following equation:

$$\delta(r,t) = \frac{\Delta}{2} \cdot \left[1 - \left(\frac{r^2}{r_c^2}\right) + \left(\frac{2 \cdot r^2}{r_c^2}\right) \cdot \ln\left(\frac{r}{r_c}\right)\right] \cdot \sin(2 \cdot \pi \cdot f \cdot t) \quad (1)$$

where:
- δ is the relative deflection of the diaphragm towards the neutral position;
- r is the radial distance from the center of the diaphragm, $r \epsilon (0, r_c]$;
- r_c is the diaphragm radius.

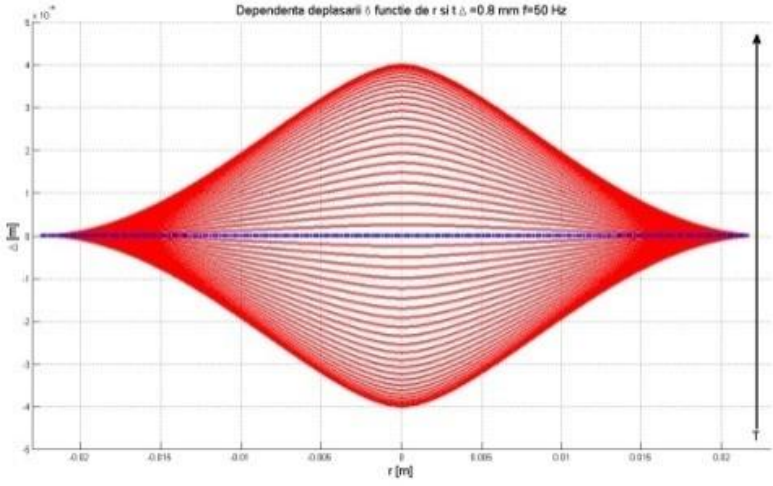

Figure 7. Dependence of displacement $\boldsymbol{\delta}$ by r and t for $\Delta = \mathbf{0.8mm}$ f=50 Hz

Differentiating equation (1) according to time is obtained the speed of oscillation of the membrane

$$\frac{\partial \delta(r,t)}{\partial t} = u(r,t) = \pi \cdot f \cdot \Delta \cdot \left[1 - \left(\frac{r^2}{r_c^2}\right) + \left(\frac{2 \cdot r^2}{r_c^2}\right) \cdot \ln\left(\frac{r}{r_c}\right)\right] \cdot \cos(2 \cdot \pi \cdot f \cdot t) \qquad (2)$$

In the case of compressible flows, applying the law of conservation of mass, the instantaneous flux of fluid passing through the orifice is given by the equation:

$$\dot{Q}_0(t) = \rho \cdot \tilde{u}_0(t) \cdot A = \rho \cdot \int_0^{r_c} u(r,t) \cdot 2 \cdot \pi \cdot r \cdot dr = \frac{\pi^2}{16} \cdot \rho \cdot \Delta \cdot f \cdot {D_c}^2 \cdot cos(2 \cdot \pi \cdot f \cdot t) \qquad (3)$$

where A is the orifice section.

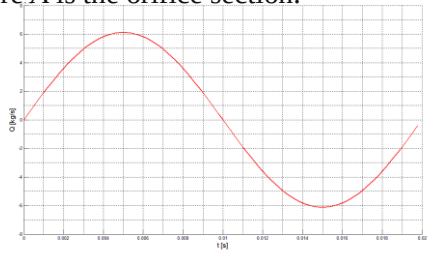

Figure 8. Dependence of fluid flux with time Δ= 0.8 mm f=50

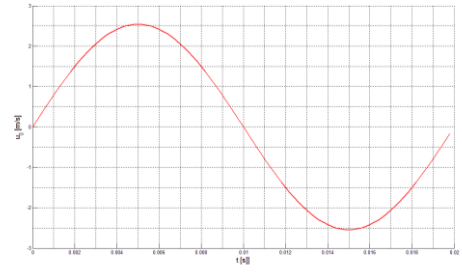

Figure 9. Instantaneous velocityΔ= 0.8 mm f=50 Hz

The fluid leaving the orifice with velocity:

$$\tilde{u}_0(t) = \frac{\dot{Q}_0(t)}{\rho \cdot A} = \frac{\pi}{4} \cdot \Delta \cdot f \cdot \left(\frac{D_c}{D_0}\right)^2 \cdot \cos(2 \cdot \pi \cdot f \cdot t) \qquad (4)$$

The velocity $\tilde{u}_0(t)$ is the fundamental criterion for estimating the performance of the jet, when no velocity profile information is available. Because $\tilde{u}_0(t)$ is independent of the orifice and cavity depth, changing of these two dimensions is irrelevant and is not taken into account in this model. The maximum velocity, $\tilde{U}_{max}$, and the mean velocity over a complete cycle, $\bar{U}_0$, can be determined from eq. 4:

$$\tilde{U}_{max} = \frac{\pi}{4} \cdot \Delta \cdot f \cdot \left(\frac{D_c}{D_0}\right)^2 \tag{5}$$

$$\bar{U}_0 = \frac{1}{T} \cdot \int_0^{T/2} \tilde{u}_0(t)dt = \frac{1}{4} \cdot \Delta \cdot f \cdot \left(\frac{D_c}{D_0}\right)^2 \tag{6}$$

where: T is the period of oscillation of the membrane.

The total fluid flux, Q_0 and the mean fluid flux, $\bar{\dot{Q}}_0$ over a complete cycle are:

$$Q_0 = \int_0^{T/2} \dot{Q}_0(t)dt = \frac{\pi}{16} \cdot \rho \cdot \Delta \cdot D_c^2 \tag{7}$$

$$\bar{\dot{Q}}_0 = \frac{Q_0}{T} = \frac{\pi}{16} \cdot \rho \cdot \Delta \cdot f \cdot D_c^2 \tag{8}$$

If $\tilde{u}_0(t)$ is used for replacing the velocity profile $u_0(r,t)$, the instantaneous momentum of the fluid flux could be approximated with the next relation:

$$\begin{aligned} \dot{M}_0(t) &= \rho \cdot \int_0^{r_c} u_0^2(r,t) \cdot 2 \cdot \pi \cdot r \cdot dr \cong \rho \cdot \tilde{u}_0^2(t) \cdot A \\ &= \frac{\pi^3}{64} \cdot \rho \cdot \Delta^2 \cdot f^2 \cdot D_0^2 \cdot \left(\frac{D_c}{D_0}\right)^4 \cdot cos^2(2 \cdot \pi \cdot f \cdot t) \end{aligned} \tag{9}$$

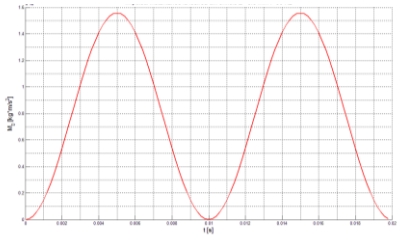

Figure 10. Instantaneous momentum Δ= 0.8 mm f=50 Hz

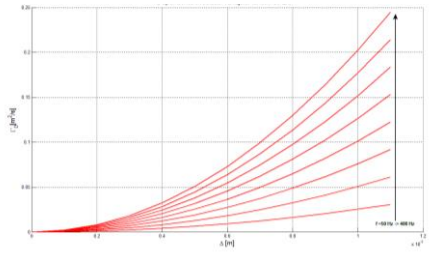

Figure 11. Vortex circulation dependence function of Δ and f

Therefore, the total momentum of the flow of fluid passing through the orifice during one complete cycle I_0 can be approximated by the following relation:

$$I_0 = \int_0^{T/2} \dot{M}_0(t)dt \cong \frac{\pi^3}{256} \cdot \rho \cdot \Delta^2 \cdot f \cdot D_0^2 \cdot \left(\frac{D_c}{D_0}\right)^4 \tag{10}$$

The next relation is used for calculation the mean momentum:

$$\bar{\dot{M}}_0 = \frac{I_0}{T} \cong \left(\frac{\pi^3}{256}\right) \cdot \rho \cdot \Delta^2 \cdot f^2 \cdot D_0^2 \cdot \left(\frac{D_c}{D_0}\right)^4 \tag{11}$$

So far there is no precise method for determining the vortex circulation Γ.

However, this circulation can be approximated using the total circulation flow vortex in the area of the outlet orifice, Γ_0. According to Glezer's [14] theory, the total circulation could be approximated using the next relation:

$$\Gamma_0 = \int \frac{u_0^2(0,t)}{2} dt \tag{12}$$

Replacing $u_0(0,t)$ with the mean velocity at the exit of orifice $\tilde{u}_0(t)$, the next relation is obtained:

$$\Gamma_0 \cong \int_0^{T/2} \frac{\tilde{u}_0^2(t)}{2} dt = \frac{\pi^2}{128} \cdot \Delta^2 \cdot f \cdot \left(\frac{D_c}{D_0}\right)^4 \tag{13}$$

IV. INTERACTION OF SYNTHETIC JETS WITH A UNIFORM FLOW ON A FLAT PLATE

Two different types of actuators are analyzed. The figure 12 shows the simple synthetic jet actuator with the nozzle normal to the airfoil surface, and the figure 13 shows the oriented synthetic jet actuator where the nozzle is tangential to the airfoil surface.

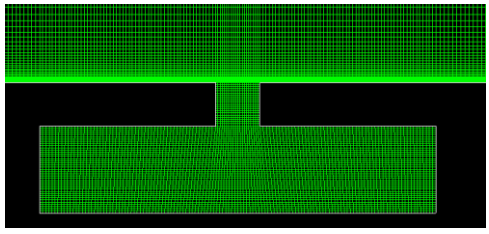

Figure 12. Normal synthetic jet actuator

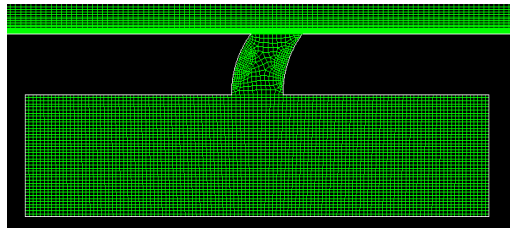

Figure 13. Directed synthetic jet actuator

Simulations are performed at a frequency of *50 Hz* and amplitude of *0.8 mm.* The inlet velocity profile is set using the well-known Blasius laminar velocity profile, as the boundary layer thickness in the actuator region to have the same dimension as the orifice diameter, *5 mm*. The fluid used in numerical simulation is air with the exterior velocity of 4 *m/s*, with the following values: density *1.225 kg/m*^{3} and viscosity *1.7894·10*$^{-5}$ *kg/m·s*.

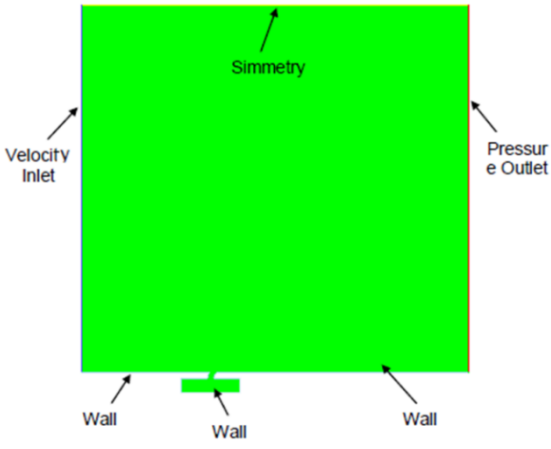

Figure 14. Computational domain and grid

Table 1 Input data

	Value
Density [kg/m^3]	1.225
Viscosity [kg/m·s]	1.7894·10^{-5}
Velocity [m/s]	4

Figure 14 shows the computational domain and the boundary condition used for the numerical simulation of this section.

There could be observed that the membrane of the actuator is represented as a wall. In order to maintain the laminar flow over the all plate, the Reynolds number must remain below the critical value $Re_{cr} = 500000$.

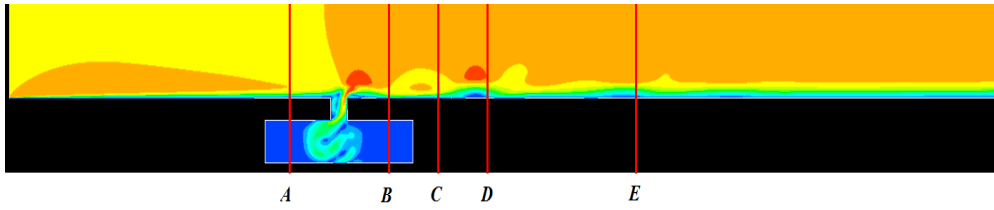

Figure 15. Velocity profile at different locations on the plate

The coordinates for each location are calculated considering the axis system with the origin at the center of the orifice: $X_A = -0.015$ m; $X_B = 0.015$ m; $X_C = 0.030$ m; $X_D = 0.045$ m; $X_E = 0.090$ m (figure 15).

A graphic comparison between the theoretical velocity profile (the Blasius velocity profile), the velocity profile perturbed by a normal synthetic jet actuator, and the velocity profile perturbed by an oriented synthetic jet actuator, is shown in the figure 16.

Location	T=0.008s	T=0.038s
A	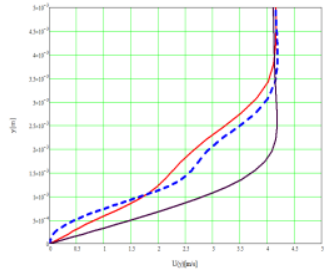	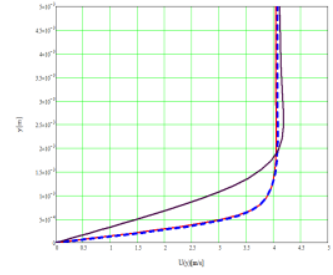
B	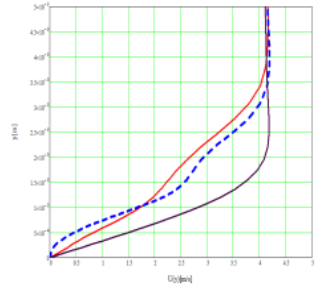	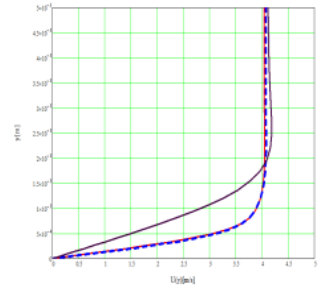
C	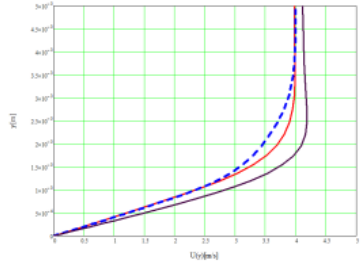	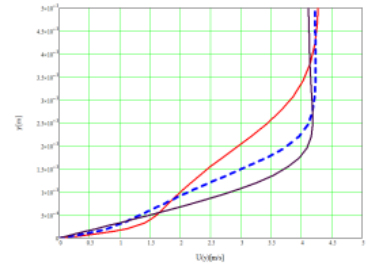

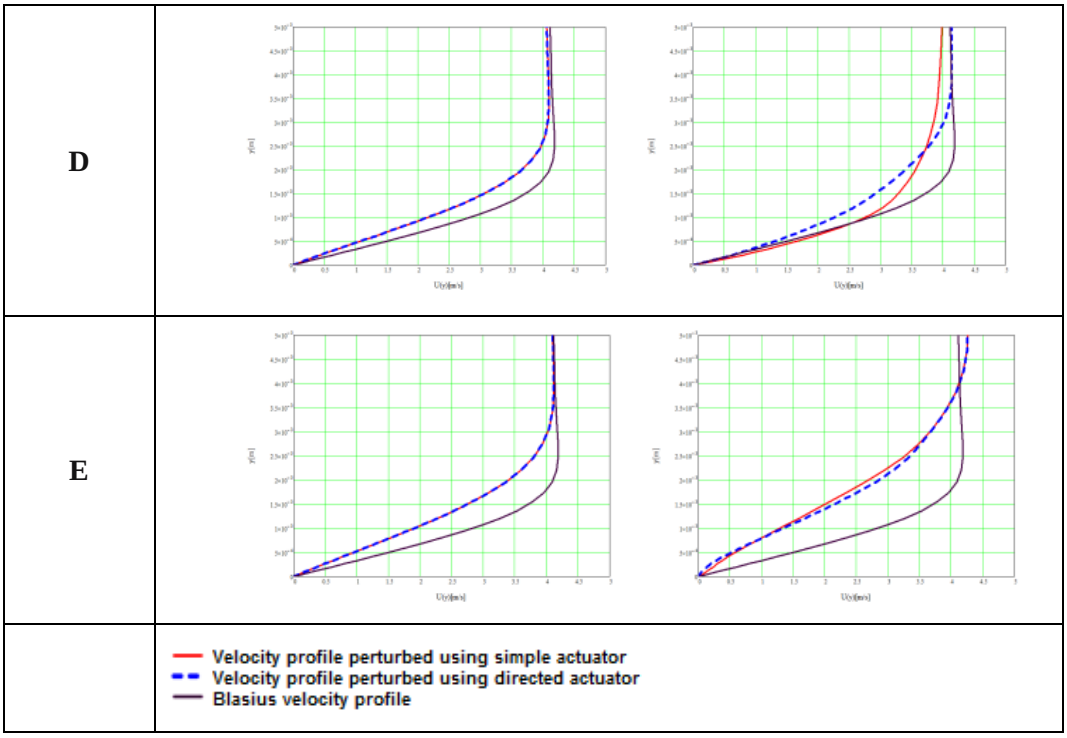

Figure 16. Velocity profile at different sections using two types of actuators

V. CONTROLLABILITY OF DYNAMIC STALL USING SYNTHETIC JETS

The phenomenon of dynamic stall is encountered in aeronautics at rotor blades. The purpose of this study is to evaluate the effect of using synthetic jet to delay the flow separation and therefore the reduction of hysteresis loop of the aerodynamic forces.

We investigated numerically the case of the NACA0012 airfoil with a chord length c =15 cm, which executes a sinusoidal pitching motion, $\alpha(t) = 10° + 15° \cdot \sin(18.67\ t)$, around the point located at ¼ c from the leading edge (corresponding to a reduced frequency $k = \frac{\omega \cdot c}{2 \cdot V_\infty} = 0.1$.

The airfoil is placed in a free uniform flow with velocity V =14 m/ s and turbulence intensity of about 1%.

The Reynolds number is $Re = 1.35 \cdot 10^5$.

For the present study, unsteady Reynolds averaged Navier-Stokes (RANS) model is the suitable approach to perform the dynamic stall flow simulations with an acceptable computational cost and, at least, reasonable accuracy.

The turbulence model used in Fluent is K-ω-SST.

The computational domain is composed by an inner circular domain which executes a rigid pitching motion around its center with angular velocity $\dot{\alpha}(t) = 15° \cdot 18.67 \cdot \cos(18.67\ t) \cdot \frac{\pi}{180}$ and a fixed exterior circular domain with radius 26 c. The hybrid grid has 760000 nodes; about 1000 nodes are placed on the airfoil surface and clustered close to leading and trailing edges.

The height of the first row of cells bounding the airfoil is set to $10^{-5} \cdot c$ which ensures $y^+ \leq 1$ for a properly resolved of viscous laminar sub layer.

The height of the cells expands with a growth factor 1.1 towards to the boundary of the airfoil geometric layer.

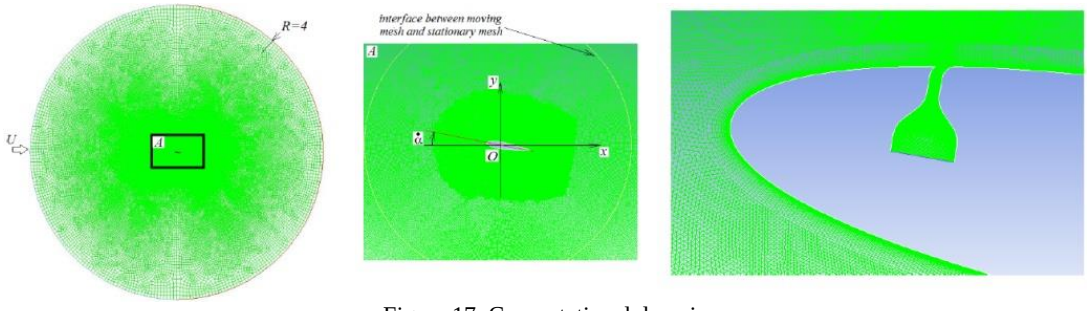

Figure 17. Computational domain

A synthetic jet actuator is placed at 15% of airfoil's chord. This control device is activated just for $t_{sj} = \frac{T}{4} \rightarrow \omega_{sj} = 747\frac{rad}{s} \rightarrow when\ \alpha > 20°$. The jet velocity in this case is $V(t) = 4 \cdot \sin\left(\omega_{sj}\left(t - \frac{T}{8}\right) - \frac{\pi}{2}\right)$.

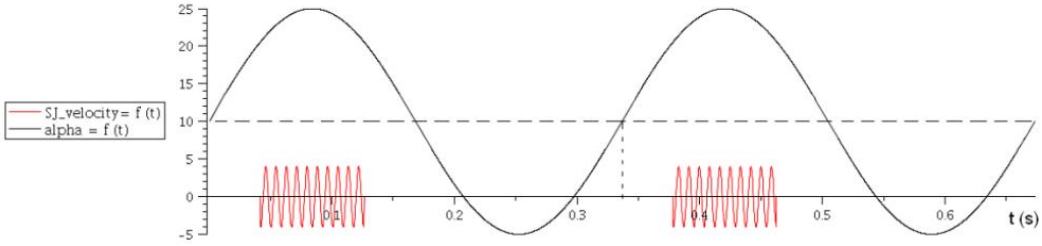

Figure 18. Times when the actuator is active

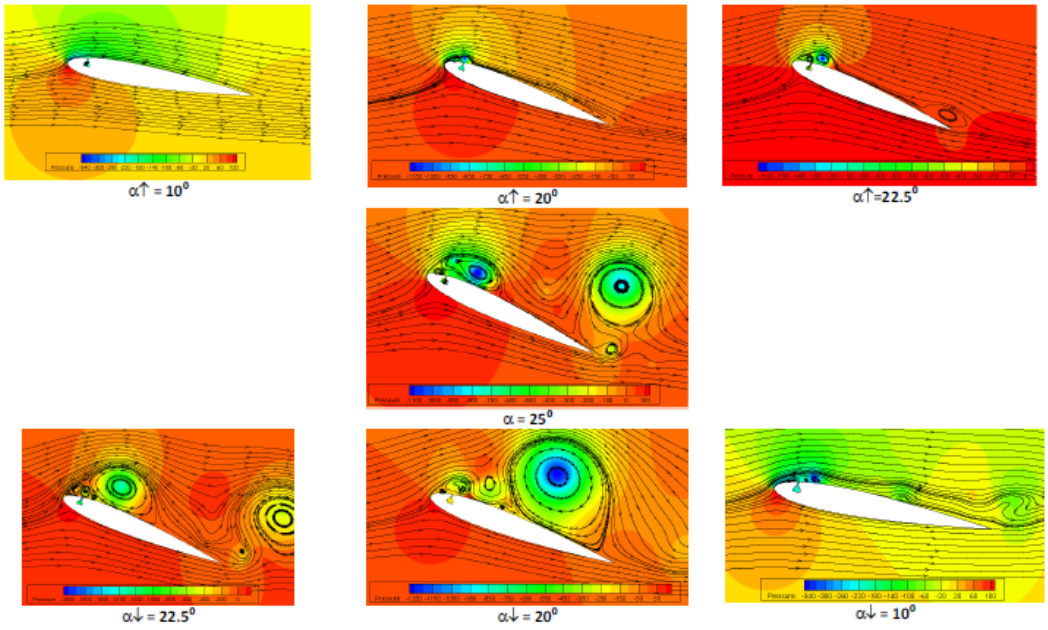

Figure 19. Streamlines and static pressure contours at different angles of attack

In Figure 19 we present streamlines over pressure contours (gauge pressure) at a few time steps in airfoil pitching motion with synthetic jet control.

We notice that the synthetic jet reduces the hysteresis of aerodynamic coefficients as seen in Figure 20(a).

The high impulse of the jet produces a quick separation of vortex generated at the leading edge and the flow becomes unstable on the upper surface.

More numerical simulations are necessary to identify an optimal position of the control device and the proper set of frequencies and amplitude for the membrane motion.

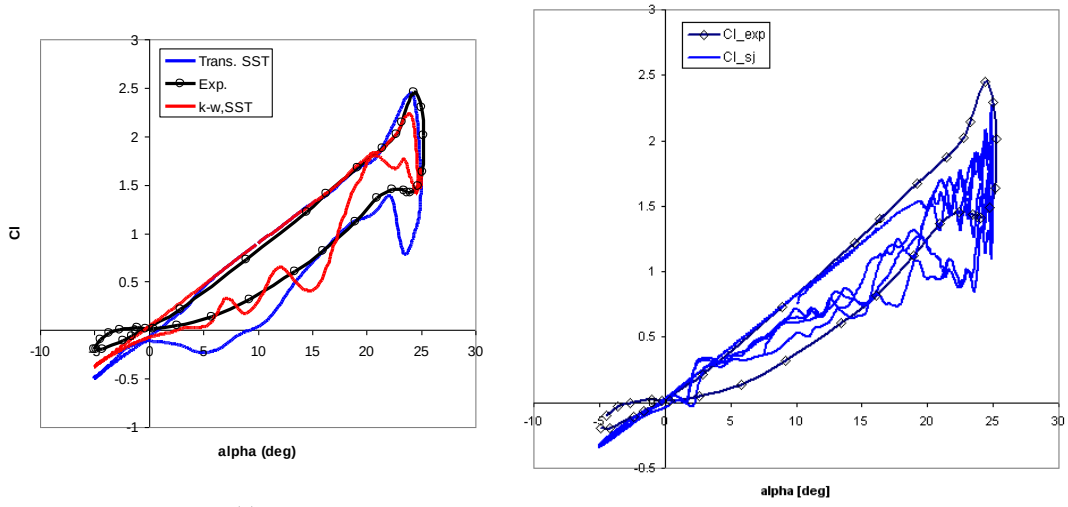

(a) (b)

Figure 20. Numerical simulations of dynamic stall phenomenon

The Figure 20(a) shows a comparison between the hysteresis lift coefficient using turbulence models K-ω-SST, Transitional SST and experimental data. The Figure 20(b) presents a comparison between the lift coefficient with synthetic jet and the experimental data without synthetic jets.

VI. CONCLUSIONS

In this paper we analyze the numerical and experimental behavior of the synthetic jets. Using ANSYS-Fluent a set of numerical simulations for eight different frequencies (50-400 Hz) and a range of five amplitudes (0.4-1.2 mm) was performed.

Using the simulations performed on a flat plate it was found that the directed synthetic jet actuator provides better results than the simple synthetic jet actuator.

From the scientific literature and the investigations conducted on synthetic jets there are found a wide range of benefits as for instance the boundary layer velocity profile thickness increase, the drag coefficient decrease, and the lift coefficient increase.

At the same time there are a number of disadvantages related to the control system maintenance, and many manufacturing issues in the case of the oriented synthetic jets.

There are a number of practical applications where the synthetic jets proved to be effective: the missiles micro jets control systems, and cooling systems with micro jets.

This paper provides a starting point for the following research projects and in the future we intend to continue the study of the active control of flow.

REFERENCES

[1] L. D. Kral (deceased), *ACTIVE FLOW CONTROL TECHNOLOGY*, ASME Fluids Engineering Division Technical Brief, Washington University St. Louis, Missouri, 2008.

[2] J. E. Green, *Laminar Flow Control – Back to the Future*?, Aircraft Research Association Ltd., Bedford UK, MK41 7PF 38th Fluid Dynamics Conference and Exhibit BR 23 - 26 June 2008, Seattle, Washington.

[3] S. Zhong, M. Jabbal, H. Tang, L. Garcillan, F. Guo, N. Wood, C. Warsop, *Towards the Design of Synthetic-jet Actuators for Full-scale Flight Conditions Part 1: The Fluid Mechanics of Synthetic-jet Actuators*, Received: 16 April 2006 / Accepted: 23 November 2006 / Published online: 2 March 2007 # Springer Science + Business Media B.V. 2007.

[4] R. Rathnasingham and K. S. Breuer, *Characteristics of Resonant Actuators for Flow Control*, AIAA Paper 96-0311, Jan. 1996.

[5] J. T.Lachowicz, C. S. Yao and R. W. Wlezien, *Scaling of an OscillatoryFlow-Control Actuator*, AIAA Paper 98-0330, Jan. 1998.

[6] M. O. Muller, L. P. Bernal, P. K. Miska, P. D. Washabaugh, T. A. Chou, B. A. Parviz, C. Zhang and K. Najafi, *Flow Structure and Performance of Axisymmetric Synthetic Jets*, AIAA Paper 2001-1008, Jan. 2001.

[7] A. Crook, *The Control of Turbulent Flows Using Synthetic Jets*, Ph.D. Dissertation, School of Engineering, Univ. of Manchester, Manchester, England, U.K., Jan. 2002.

[8] D. P. Rizzetta, M. R. Visbal and M. J. Stanek, Numerical Investigation of Synthetic-Jet Flowfields, *AIAA Journal*, Vol. **37**, No. 8, pp. 919–927, 1999.

[9] C. Y. Lee and D. B. Goldstein, Two-Dimensional Synthetic Jet Simulation, *AIAA Journal*, Vol. **40**, No. 3, pp. 510–516, 2002.

[10] Y. Utturkar, R. Mittal, P. Rampunggoon and L. Cattafesta, *Sensitivity of Synthetic Jets to the Design of the Jet Cavity*, AIAA Paper 2002-0124, Jan. 2002.

[11] J. M. Shuster and D. R. Smith, *A Study of the Formation and Scaling of a Synthetic Jet*, AIAA Paper 2004-0090, Jan. 2004.

[12] H. Tang and S. Zhong, 2D Numerical Study of Circular Synthetic Jets in Quiescent Flows, *Aeronautical Journal*, Vol. **109**, No. 1092, pp. 89–97, 2005.

[13] S. Timoshenko and S. Woinowsky-Krieger, *Theory of Plates and Shells*, 2nd ed., McGraw–Hill, London, pp. 67–69, 1959.

[14] A. Glezer, The Formation of Vortex Rings, *Physics of Fluids*, Vol. **31**, No. 12, pp. 3532–3542, 1988.

[15] N.Didden, On the Formation of Vortex Rings: Rolling-Up and Production of Circulation, *Zeitschrift f˙ur Angewandte Mathematik und Physik*, Vol. **30**, pp. 101–106, Jan. 1979.

[16] S. Zhong, H. Tang, Incompressible Flow Model of Synthetic Jet Actuators, *AIAA Journal* (Impact Factor: 1.08). 01/2006; **44**(4): 908-912, DOI:10.2514/1.15633, University of Manchester

[17] D. C. McCormick, *Boundary layer separation control with directed synthetic jets*, AIAA 2000-0519, United Technologies Research Center, 1999.

[18] R. Duvigneau, A. Hay & M. Visonneau, Optimal location of a synthetic jet on an airfoil for stall control, *Journal of Fluids Engineering*, Vol. **129**, No 7, pp. 825-833, July 2007.

[19] F. Frunzulica, A. Dumitrache, H. Dumitrescu and O. Preotu, *Flow control of separating boundary layer on the Coanda surface*, POLITEHNICA" University of Bucharest, Faculty of Aerospace Engineering.

[20] *** ANSYS *FLUENT* 12.0 User's *Guide*

[21] F.Frunzulica, A. Dumitrache, O. Preotu, H. Dumitrescu, *Active and passive control methods on the aerodynamic surfaces*,The 35th Annual Congress of the American Romanian Academy of Arts and Sciences (ARA35), July 6-10, 2011 , Timisoara – ROMANIA (Proceedings), (The 35th Annual Congress of the American Romanian Academy of Arts and Sciences - Proceedings, pp. 171-174, ISBN 978-2-553-01596-0).

[22] F. Frunzulica, A. Dumitrache, H. Dumitrescu and O. Preotu, *Active control of separating boundary layer on the Coanda surface*, 4th European Conference for Aerospace Sciences, EUCASS 2011, Sankt-Petersburg, Russia, July 4, 2011 – July 8, 2011 (Technical reports. Conference Proceedings), (Technical report EUCASS 612-04-2011).

[23] F. Frunzulica, H. Dumitrescu, R. Mahu and O. Preotu, *Active and Passive Lift Force Augmentation Techniques on Wind Turbines*, 9th International Conference of Numerical Analysis and Applied Mathematics – ICNAAM 2011, Halkidiki, Greece, 19-2 September 2011 (American Institute of Physics Proceedings ISBN 978-0-7354-0954-5), AIP Conf. Proc. 1389, pp. 1507-1510; doi:10.1063/1.3637911 (4 pages), NUMERICAL ANALYSIS AND APPLIED MATHEMATICS ICNAAM 2011, Date: 19–25 September 2011.

[24] M. Amitay, A. M. Honohan, M. Trautman and A. Glezer, *Modification of the aerodynamic characteristics of bluff bodies using fluidic actuators*, 28th AIAA Fluid Dyn. Conf. 97-2004, Snowmass, Colo., 1997.
[25] A. Glezer and M. Amitay, Synthetic Jets, *Rev. Fluid Mech*. **34**:503–29., 2002.
[26] B. L. Smith, A. Glezer, Vectoring of a high aspect ratio air jet using zero-net-mass-flux control jet, *Bull. Am. Phys. Soc*.**39**: 1894, 1994.
[27] F. J. Chen, G. B. Beeler, R. G. Bryant, R. L. Fox, *Development of synthetic jet actuators for active flow control at NASA Langley*, AIAA Fluids Meet. 2000-2405, Denver, Colo., 2000.
[28] R. Mahalingam, N. Rumigny, A. Glezer, *Thermal management using synthetic jet ejectors*, Components and Packaging Technologies, IEEE Transactions, Volume **27**, 3: 439-444., 2004.